Green Chemistry

RSC Publishing

PAPER

View Article Online
View Journal | View Issue

Dissolution of feather keratin in ionic liquids†

Cite this: *Green Chem.*, 2013, **15**, 525

Azila Idris,*[a,b] R. Vijayaraghavan,[a] Usman Ali Rana,‡[a] Dale Fredericks,[c] A. F. Patti[a] and D. R. MacFarlane[a]

Received 2nd October 2012,
Accepted 13th December 2012

DOI: 10.1039/c2gc36556a

www.rsc.org/greenchem

Keratin from various livestock industries is currently a waste material that has potential as a source of polyamide polymers that could replace fossil fuel derived materials if processing methods can be developed. In this work we have investigated methods for the dissolution and regeneration of keratin. Dissolution of keratin (from turkey feather) in ionic liquids was conducted under nitrogen at 130 °C for 10 hours. It was found that [BMIM]Cl, [AMIM]Cl and [choline][thioglycolate] could dissolve turkey feather keratin without addition of solvent or other chemicals. A significant percentage of solubility was obtained, up to 45% by weight. A water insoluble fraction was recovered by addition of water to the solution (~50%). The structure and properties of this regenerated, water insoluble fraction were investigated. Compared to the starting material, the regenerated keratin shows structural changes rather than chemical changes within the polypeptide chains. The remaining fraction, consisting of water soluble fragments, was characterised by gel electrophoresis.

1. Introduction

Keratin is a fibrous protein that can be found in feather, wool, human hair, finger nails, animal claws and horn.[1,2] These biopolymers are plentifully available as a by-product from poultry production and textile industries.[3–5] However this kind of protein is not easy to dissolve or extract because keratin is bound by strong internal interactions that stabilise the protein structure.[4,6] In order to utilise these biopolymers and convert them to usable materials there is a need for alternative solvents that are efficient in dissolving keratin and preserving, at least in part, the protein structure. The main objective of the present study therefore is to investigate the use of ionic liquids (ILs) in the dissolution and regeneration of keratin, in particular utilising the unique solvency characteristics and high temperature properties of ILs. Feathers are about 90% keratin[7] which contains about 7% of cysteine.[8,9] Feather proteins are insoluble in normal organic solvent due to the tight packing of the α-helix and β-sheet in the polypeptide chain. Additionally, a high degree of crosslinking of the polypeptide chain is affected by cysteine residues which participate in disulfide bridge formation.[6,8,10] In order to extract the keratin, cleaving the disulfide bonds can be achieved by reduction,[11–13] oxidation,[12–14] sulfitolysis[13,15] or oxidative sulfitolysis.[13,16] Even though many reagents have the capability to reduce the disulfide bonds, only a few, such as thiols[17] and ammonium bisulfite, have the required ability and reactivity to preserve and maintain the protein structure. However, these materials are difficult to recycle, often toxic and costly to produce.

Ionic liquids (ILs) are generally defined as salts which are liquid below 100 °C and comprised entirely of cations and anions.[18,19] They offer a unique combination of properties as solvents including in some cases low vapour pressure and high thermal stability.[20] The hydrophobicity/hydrophilicity of ionic liquids can be altered by manipulating the structures of the cations and anions.[21] In recent years, a number of ionic liquids have been identified as solvents for the dissolution of biopolymers such as cellulose, starch, wood, lignin, feather and wool. These are generally insoluble in organic solvents but show a reasonable solubility in certain ionic liquids.[4,22–28] Duck feather keratin, for example, was found to be soluble in the ionic liquids (1-butyl-3-methylimidazolium chloride [BMIM]Cl and 1-allyl-3-methylimidazolium chloride [AMIM]Cl).[29] The same ionic liquids have been found to be useful for wool dissolution by Xie *et al.*[4] [BMIM]Cl was also found to be useful in the synthesis of wool keratin/cellulose composite materials. The materials displayed a homogeneous structure and did not show a residual fiber structure.[4] Therefore, the dissolution of biopolymers using ionic liquids provide

[a]*School of Chemistry, Faculty of Science, Monash University, Clayton, VIC 3800, Australia*
[b]*Department of Chemistry, Faculty of Science, University of Malaya, 50603 Kuala Lumpur, Malaysia*
[c]*ARC Special Research Centre for Green Chemistry, Monash University, Clayton, VIC 3800, Australia. E-mail: azila.idris@monash.edu.au, azilaidris@um.edu.my*

†Electronic supplementary information (ESI) available. See DOI: 10.1039/c2gc36556a

‡Current address: Sustainable Energy Technologies (SET) center, College of Engineering, King Saud University, PO Box 800, Riyadh 11421, Kingdom of Saudi Arabia.

possibilities for the utilisation and conversion of biopolymers into useful materials with great potential in industrial applications.

In the current study we have used [BMIM]Cl, [AMIM]Cl, as well as novel ionic liquids containing a thiol functional group [choline][thioglycolate] and [bis-(2-ethylhexyl)ammonium]-[thioglycolate] as possible disulfide bridge reducing, or exchange reagents, to dissolve and regenerate the keratin in turkey feather. A combination of analytical techniques including ATR-FTIR, XRD, solid state NMR, TGA, DSC and gel electrophoresis has been used to investigate the extent of keratin solubility in these ionic liquids and the physiochemical properties of the regenerated keratin material. We show that a significant amount of keratin (approximately 45–50 wt%) can be dissolved in the above mentioned ionic liquids.

2. Experimental

Materials preparation

The cleaned turkey feathers used in the experiments were commercial materials supplied by Shamrockcraft, purchased from Spotlight, Clayton, Australia. Only barbs of the turkey feathers were used in the experiments. 1-Butyl-3-methylimidazolium chloride ([BMIM]Cl, 98% of purity) was purchased from Sigma Aldrich. All other ionic liquids were prepared in-house for this project as described further below. For the preparation of these ionic liquids, allylchloride (98%), *N*-methylimidazole (99%), choline hydroxide (20 wt% in H_2O), thioglycolic acid (98%) and bis-(2-ethylhexyl)amine (99%) were obtained from Sigma Aldrich. For NMR analysis, deuterated chloroform ($CDCl_3$) and deuterated methanol (CD_3OD) purchased from Merck was used. Unless otherwise stated, all other organic solvents and reagents were used as received from commercial suppliers.

Attenuated total reflectance-Fourier transform infrared spectroscopy (ATR-FTIR)

Fourier transform infrared spectra were obtained using a Bruker IFS Equinox FTIR system coupled with a Golden Gate single bounce diamond micro-Attenuated total reflectance crystal and a liquid nitrogen cooled Mercury/Cadmium Telluride detector. The FTIR was performed in the wavenumber range of 600 cm^{-1} to 4000 cm^{-1}. The spectra were recorded with a resolution of 4 cm^{-1} with 50 scans. Spectra were baseline corrected.

Powder X-ray diffraction (PXRD)

The powder X-ray diffraction (PXRD) patterns were obtained at 22 ± 2 °C using a Sietronics powder diffractometer. For each XRD experiment, approximately, 1–2 g of the finely ground sample was placed randomly on a locally designed flat brass sample holder fitted with an o-ring sealed covered Mylar sheet providing an airtight atmosphere. CuKα1 radiation (λ = 1.540 Å) was produced at 40 kV and 25 mA. The data were collected in the Brag–Brentano ($\theta/2\theta$) horizontal geometry using a 2θ-range of 5 to 50.0° (2θ) range with a step size of 0.02° 2θ and an accompanying scan rate of 0.5° min^{-1}.

Nuclear magnetic resonance spectroscopy (NMR)

^1H NMR and ^{13}C NMR spectra were recorded at 400 MHz on a Bruker DPX-400 spectrometer. All samples were measured as solutions in deuterated chloroform and methanol. Chemical shifts are reported in ppm on the δ scale, and the coupling constant is given in Hz. Chemical shifts were calibrated on the solvent peak unless otherwise specified. Solid state 1D ^1H static NMR spectra of neat and regenerated samples were acquired at a Larmor frequency of 300 MHz on a Bruker AV-300 spectrometer. The ^{13}C CP MAS NMR spectra of these samples were acquired using a 4 mm rotor with Kel-f cap at 10 kHz spinning rate. The contact time in the CP MAS experiments was 2.4 ms with a recycle delay of 1 s and cw decoupling. The number of scans was ~90 000 to 100 000. In the case of 1D ^1H static NMR experiments, the pulse length was ~3.6 μs with a recycle delay of 5 s and 16 to 20 scans.

Thermogravimetric analysis (TGA)

The thermal stability of the original and regenerated materials were investigated by TGA using a Pyris 1 in a flowing dry argon atmosphere between 25 and 700 °C at a heating scan rate of 10 °C min^{-1}. The instrument was calibrated using four reference materials, alumel, perkalloy, iron and nickel. The samples were first dried under vacuum in an oven at a temperature of 70 °C. These samples were then loaded in ceramic pans and equilibrated for 15 minutes at the starting temperature of 25 °C before running each experiment.

Differential scanning calorimetry (DSC)

Differential scanning calorimetry (DSC) was conducted on a DSC Q100 series from TA Instruments with 5–10 mg of sample in closed aluminium pans, at a ramp rate of 10 °C per minute. All samples were cooled to −150 °C, held for 5 minutes and heated to 200 °C. Thermal scans below room temperature were calibrated *via* the cyclohexane solid–solid transition and melting point at −87.0 °C and 6.5 °C respectively. Thermal scans above room temperature were calibrated using indium, tin, lead and zinc with melting points at 156.6 °C, 231.9 °C and 419.5 °C respectively. Transition temperatures are reported using the peak maximum of the thermal transition.

Electrospray ionisation mass spectrometry (ESI-MS)

Electrospray ionisation mass spectra were recorded on a Micromass Platform II API QMS Electrospray Mass Spectrometer. Samples dissolved in methanol were subjected to a suitable cone voltage, usually 25 V to 35 V. Measurements were made in both the positive and negative modes.

SDS-PAGE electrophoresis

Protein samples were diluted in 4× NuPAGE® loading buffer (Life Technologies) and electrophoresed using the Hoefer miniVE vertical electrophoresis system (Amersham Biosciences) in 4–12% Bis-Tris NuPAGE® gradient gels (Life

Technologies). Proteins were stained and visualised by silver staining.

Preparation of ionic liquids

1-Allyl-3-methylimidazolium chloride [AMIM]Cl was prepared according to the literature[30] as described in more detail in the ESI.† Structural confirmation of the ionic liquids obtained was carried out by spectroscopic methods including ^{1}H NMR and mass spectroscopy (electrospray ionisation). As contaminants have been shown to affect the physical properties of ILs,[31,32] water content was determined by Karl Fischer titration.

Apart from imidazolium salts, a series of thioglycolate ionic liquids were also synthesised. The reaction is a simple acid–base neutralisation which involved transferring a proton from a Bronsted acid to a Bronsted base without the use of any solvent.[19] In this investigation, bis-2-ethylhexylammonium hydroxide and choline hydroxide were combined with one equivalent of thioglycolic acid, respectively. These chemical reactions are highly exothermic, therefore an ice bath was used to control the temperature throughout the chemical reaction. Further details are as follows.

[Choline][thioglycolate]. Choline hydroxide (15.17 ml, 0.026 moles) was initially placed in a three-necked flask and equipped with a reflux condenser and a dropping funnel. An equimolar amount of thioglycolic acid (1.82 ml, 0.026 moles) was then added dropwise to the base while stirring rapidly in an ice bath. A viscous liquid (Scheme 1) was obtained after evaporation of the water by-product using a rotary evaporator. (4.57 g, 91%); ^{1}H NMR (ppm, 400 MHz, DMSO) δ_H: ^{1}H NMR (ppm, 400 MHz, DMSO) δ_H: 4.49 (1H, broad s, OH), 3.84 (2H, q, CH_2), 3.44 (4H, m, $2CH_2$), 3.12 (9H, s, $3CH_3$), 1.92 (1H, s, SH); ES-MS: ES^+ m/z 104.1 [choline]$^+$. ES^- m/z 90.9 [thioglycolate]$^-$. Water content (Karl Fischer): 18 034 ppm.

[Bis-(2-ethylhexyl)ammonium][thioglycolate]. Bis-(2-ethylhexyl)-amine (7.48 g, 30.9 mmoles) was loaded into a three-necked flask and equipped with a reflux condenser under vigorous stirring with a magnetic stirrer. An equimolar amount of thioglycolic acid (2.72 g, 29.5 mmoles) was then added dropwise to the flask. The flask was placed in an ice bath. Evaporation of water gave [bis-(2-ethylhexyl)ammonium][thioglycolate], a colourless liquid (Scheme 2) (9.8 g, 98%); ^{1}H NMR (ppm, 400 MHz, $CDCl_3$) δ_H: 7.23 (2H, broad s, $^+NH_2$), 3.57 (2H, s, CH_2), 2.74 (4H, d, J = 6.4 Hz, $2CH_2$), 1.73 (2H, m, 2CH), 1.27 (17H, m, $8CH_2$, SH), 0.804 (12H, m, $4CH_3$); ES-MS: ES^+ m/z 242.3 [bis-(2-ethylhexyl)ammonium]$^+$. ES^- m/z 90.9 [thioglycolate]$^-$. Water content (Karl Fischer): 8698 ppm.

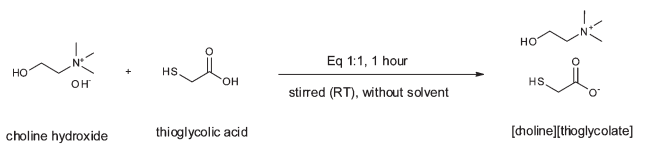

Scheme 1 Preparation of [choline][thioglycolate].

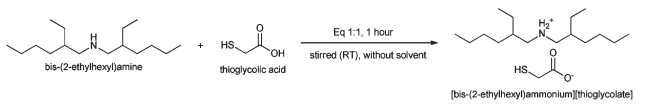

Scheme 2 Preparation of [bis-(2-ethylhexyl)ammonium][thioglycolate].

Keratin solubility

The solubility experiments were conducted in glass vials, which were fitted into a heating block under an inert atmosphere of N_2. To quantify the solubility, small incremental amounts of feather material (5 wt%) were gradually added to the ionic liquid (1 g) and mechanically stirred until they were completely dissolved in the ionic liquid. Initially it was observed that the dissolution of turkey feather occurred rapidly. Then the dissolution rate decreased as the viscosity of the turkey feather solution increased. Complete dissolution was assumed to have occurred when the feather could not be visually detected and the ionic liquid solvent remained transparent in the glass vial. A laser beam was used to more sensitively detect the presence of small particles *via* light scattering. The dissolution was run at 130 °C for 10 hours.

3. Results and discussion

Dissolution of keratin in ionic liquids

Keratin was dissolved in two series of ionic liquids which consisted of the imidazolium and thioglycolate systems. These studies were undertaken in order to determine the main properties involved in the dissolution process, for example, the effect of the structure and composition of ionic liquids on their dissolving capability. Initially, the dissolution of turkey feather was attempted at room temperature and 65 °C. Partial dissolution was observed at 65 °C. At 130 °C, complete dissolution was clearly observed. This could be due to the keratin structures at some level becoming unfolded at the elevated temperature,[33] hence permitting more interaction between keratin and the ionic liquids. According to Xie *et al.*,[4] temperature has a strong effect on the solubility and at 130 °C, better solubility of wool keratin was noted. Therefore, based on this study, the temperature was maintained at 130 °C in order to minimize any potential protein degradation and prevent any decomposition of the ionic liquids. The keratin that dissolved completely in ionic liquids resulted in a viscous solution. There was no precipitation observed after the dissolution process or after cooling to room temperature.

Table S1 in the ESI† and Fig. 1 show the limiting solubility in weight percentage of keratin in [BMIM]Cl, [AMIM]Cl, [choline][thioglycolate]. The limiting solubility was found to be around 50 wt% in all of these cases. This was determined through the sequential addition of the feather material until the solution became too viscous for rapid dissolution at 130 °C. It is likely that the true solubility is even higher than indicated here. It is interesting to note that the chloride ion seems to be as effective as the thioglycolate ion in dissolving the keratin. In the chloride case, this high solubility is

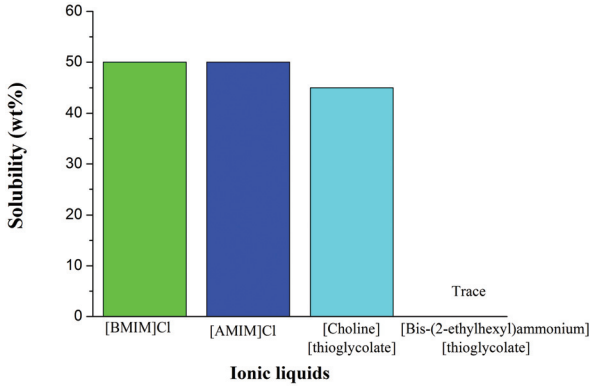

Fig. 1 Solubility of turkey feather keratin in ionic liquids.

presumably related to the ability of the ionic liquid chloride ion to disrupt hydrogen bonding in the keratin material, similar to the understanding that has emerged on the role of Cl^- in cellulose and other biopolymer dissolution in ionic liquids.[22,26,28,34] Gillespie and Lennox[35] demonstrated that alkaline thioglycolate solutions could be used to reduce the disulfide bonds in the dissolution of wool, however there was no significant increase in feather solubility observed in [choline][thioglycolate], compared to [BMIM]Cl and [AMIM]Cl. This suggests that disulfide cleavage is not a significant factor in the solubility *limit* of this type of keratin.

No dissolution was observed for turkey feather in [bis-(2-ethylhexyl)ammonium][thioglycolate]. This is probably due to the longer chain of the cation which can therefore only penetrate into the keratin network with difficulty. In addition, the viscosity of [bis-(2-ethylhexyl)ammonium][thioglycolate] is much higher compared to [choline][thioglycolate], thus decreasing the solvating properties of the ionic liquid. This compound is also the only classical protic ionic liquid of the group studied and may be prone to the proton transfer problems that have been widely discussed with respect to protic ionic liquids. The ΔpK_a of this acid–base pair is ~7.2 which has been suggested as being sufficient for strong proton transfer with regard to primary amines, but insufficient for many tertiary amine based ILs.[36]

Fig. 2 shows the keratin–[AMIM]Cl solution after returning to room temperature. At this point the solution was a very viscous, clear liquid.

Fig. 3 shows the rate of dissolution of turkey feather in [BMIM]Cl, [AMIM]Cl and [choline][thioglycolate]. Dissolution in [choline][thioglycolate] was visually slightly more rapid in the first ~10 minutes compared to the other two ionic liquids, suggesting that the initial cleavage of the disulfide bridges can accelerate the process but that the difference becomes minimal at later times. Since little is known about the disulfide bridge under these conditions, it is important to recognise that there are a number of cleavage reactions possible,[12–15,37,38] including exchange, homolytic cleavage as well as further oxidative processes if sufficient oxygen is present. In order to probe the reactions possibly taking place

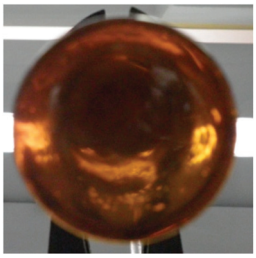

Fig. 2 Dissolved feather keratin in [AMIM]Cl.

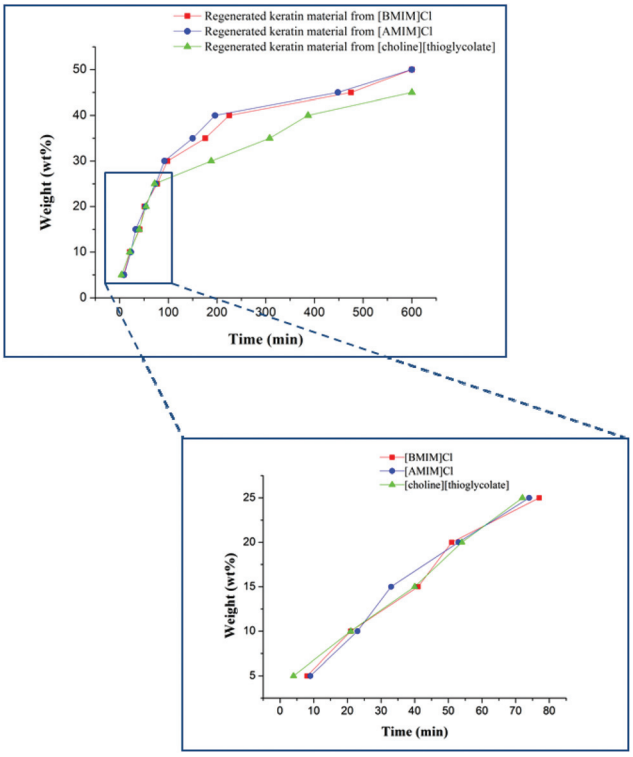

Fig. 3 Rate of dissolution of feather keratin in ionic liquids.

in the thioglycolate case, the interconversion of model compounds cystine and cysteine were studied in the thioglycolate ionic liquid. Neat cystine was added to choline thioglycolate ionic liquids and heated to 130 °C for about 5 hours. The resulting mixture was analysed by ^{13}C NMR, showing 2 new peaks in the region of 170 ppm. Cysteine dissolved in ionic liquid showed a single peak at 170 ppm. These observations seem to indicate partial cleavage or exchange of the cystine S–S bridge to form cysteine as well as the exchange product, as is also suggested by the NMR data of the regenerated keratin discussed further below.

Regenerated keratin from ionic liquids

After the keratin was dissolved, it was precipitated from the solution by addition of water at room temperature. The regenerated keratin was separated by centrifugation for 20 minutes at 5000 rpm, then dried under vacuum at 60 °C for 3 days. The

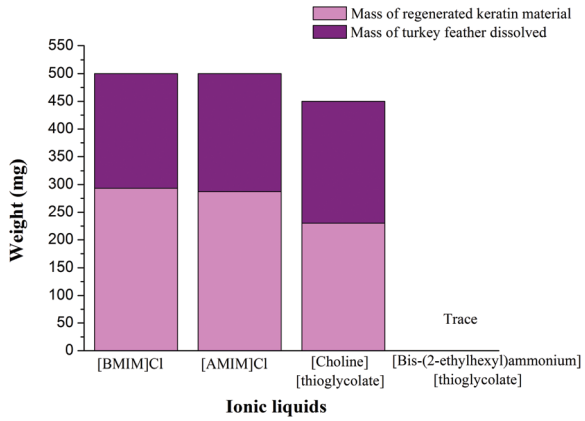

Fig. 4 Recovery of water insoluble fraction of IL dissolved keratin.

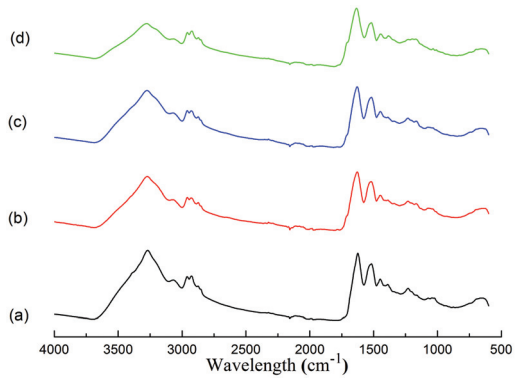

Fig. 5 ATR-FTIR spectra of (a) raw material and regenerated keratin material from (b) [BMIM]Cl, (c) [AMIM]Cl, and (d) [choline][thioglycolate].

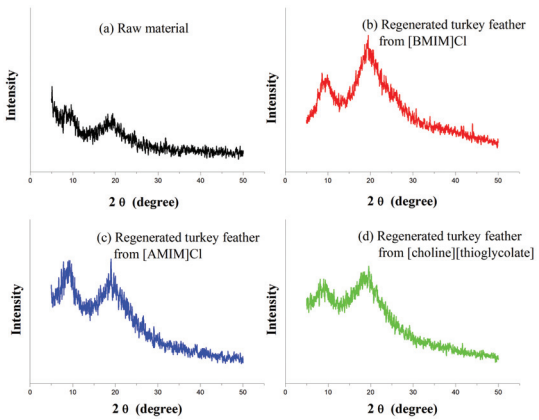

Fig. 6 XRD of (a) raw material and regenerated keratin material from (b) [BMIM]Cl, (c) [AMIM]Cl, and (d) [choline][thioglycolate].

regenerated keratin material was a fawn-coloured hard solid. Table S2 of the ESI† and Fig. 4 show the masses obtained of the regenerated aqueous-insoluble fraction. It has been reported that feather keratin consists of approximately 40% hydrophilic and 60% hydrophobic groups in the amino acid sequence.[8] Therefore, it was suggested that some of the dissolved keratin is insoluble in water and the other part of the dissolved material might be cleaved into smaller constituent polypeptide subunits which may be water soluble. Gel electrophoresis analysis was employed to further investigate the soluble component in the water–ionic liquid mixture produced during the regeneration step, as discussed further below.

Characterisation of regenerated keratin

ATR studies. In order to further understand the nature of the water insoluble keratin material regenerated from the ionic liquids, ATR-FTIR measurements were used. Infrared absorption spectra of the raw material and regenerated fraction (Fig. 5) showed characteristic absorption bands that are typically assigned to the peptide bonds (–CONH). These spectra provide information as to the orientation of the constituents and the conformation of the polypeptide chains. The Amide A vibrations of the peptide bond show medium absorption bands at 3273 cm^{-1} due to the N–H stretching. A strong absorption band was also observed at 1627 cm^{-1} and this was attributed to C═O (Amide I). A strong absorption peak at 1515 cm^{-1} was attributed to C–N stretching and N–H bending vibrations (Amide II). A weak band was observed at 1236 cm^{-1} which was due to the C–N and C–O stretching, N–H and O═C–N bending vibration (Amide III).[39,40] It can be seen that the spectra are similar to the original starting material and there are no signatures of new functional groups appearing in the regenerated material. However, in view of NMR results (below), it appears that there are chemical changes occurring due to the breaking of disulfide linkages and hydrogen bonds, which cannot be observed clearly in the ATR spectra. Therefore dissolution in these ionic liquids does not strongly affect the peptide bonds.

XRD studies. Raw material and the regenerated keratin material were examined by X-ray diffraction (XRD). In Fig. 6, the XRD patterns are compared. These figures show crystallinity in the feather keratin fibers from the substantial 2θ peak at about 9° (0.98 nm) which has been assigned to both α-helix and β-sheet structures.[41,42] The peak at about 17.8° (0.51 nm) corresponds to the diffraction pattern of the α-helix whereas the peak at about 19° (0.47 nm) is typical of the β-sheet structure.[41,42] However, due to the overlapping signals at about 17.8° and 19° from the α-helix and β-sheet, both are unable to be unambiguously assigned. It can be seen from Fig. 6 that the regenerated keratin exhibits similar diffraction patterns, indicating regeneration of the crystallinity of the original keratin. However, the peaks at about 9° and 19° are both significantly stronger in the regenerated material, suggesting a greater content of the β-sheet structure. These results are consistent with the ^{13}C CP MAS NMR spectra discussed further below.

Solid state NMR studies. Solid state ^{13}C NMR was conducted on the raw material and the regenerated keratin material to investigate the local structure and dynamics of the keratin molecules. Fig. 7 displays the ^{13}C CP MAS NMR spectra

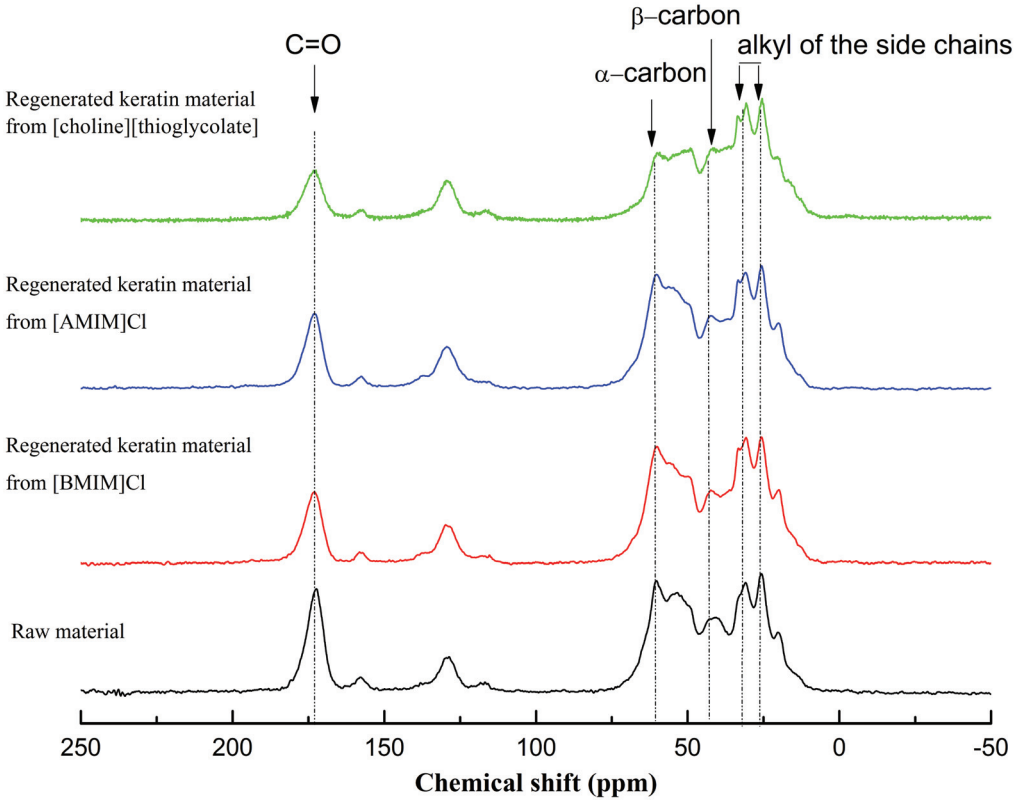

Fig. 7 The ^{13}C CP MAS NMR spectra of (a) raw material, (b) regenerated keratin material from [BMIM]Cl, (c) regenerated keratin material from [AMIM]Cl, and (d) regenerated keratin material from [choline][thioglycolate].

of keratin materials. All spectra in Fig. 7 display a distinct asymmetric peak with maxima centred between 172 and 174 ppm.

This peak corresponds to the carbonyl carbons present in keratin. The peak at 130 ppm is ascribed to the aromatic species present in the keratin.[43] All NMR spectra in Fig. 7 display this aromatic peak, which suggests that the aromatic group containing amino acid sequences are retained in the regenerated materials. The peak at 54 ppm is related to the α-carbons, while the one at 40 ppm is ascribed to the β-carbons present in leucine and cysteine residues.[44] The carbon peaks at about 30 ppm to 40 ppm are attributed to the carbon present in the proline, glutamic acid and glutamine residues. The NMR peaks at low chemical shift centred at 20 ppm, 25 ppm and 31 ppm, in addition to the peak as a shoulder at 17 ppm correspond to the alkyl groups of the side chains.[44] A peak at ~20 ppm is somewhat reduced in the thioglycolate case – this region is associated with the δ-carbon of leucine residues.[44]

Reductive cleavage of disulfide bridges associated with cysteine is expected to reduce the β-carbon signal at 40 ppm and produce a thiol signal around 25–29 ppm.[44] The two chloride cases show distinct peaks at 40 ppm that are similar to the raw material, suggesting substantial retention of disulfide bridges in these cases. In the thioglycolate case a peak remains evident, although less distinct. An exchange reaction in the thioglycolate case could produce a new S–S bridge which would also produce resonances near 40 ppm; therefore it appears likely that some sulfide exchange has taken place.

Since, the alkyl groups and the reduced cystine groups (*i.e.*, cysteine groups) display peaks in the same chemical shift range around 25–29 ppm, it is hard to distinguish the reduced cysteine uniquely in these spectra.

The two regenerated materials from [BMIM]Cl and [AMIM]-Cl display NMR spectra that are not very different from the original keratin, while the [choline][thioglycolate] material shows clear differences in the 50–65 ppm region. This is possibly because of disruption due to the reductive cleavage of the disulfide linkages.

The secondary structure of keratin, which consists of α-helix and β-sheets, produces a slightly different chemical shift of the carbonyl group in the NMR spectrum.[43,44,46] Thus the estimated percentage fraction of the α-helix and the β-sheet can be estimated by the deconvolution of the C═O peak. Fig. 8 displays the deconvoluted carbonyl NMR peaks of raw and regenerated materials. The full width at half maximum (FWHM) of the peak also provides information about the degree of motional freedom possessed by the nuclei. The higher value of full width at half maximum (FWHM) shows that the nuclei possess lower motional freedom. Previous studies showed that such deconvolutions usually result in two peaks, one at 175.6 ± 0.2 ppm, which is ascribed to the

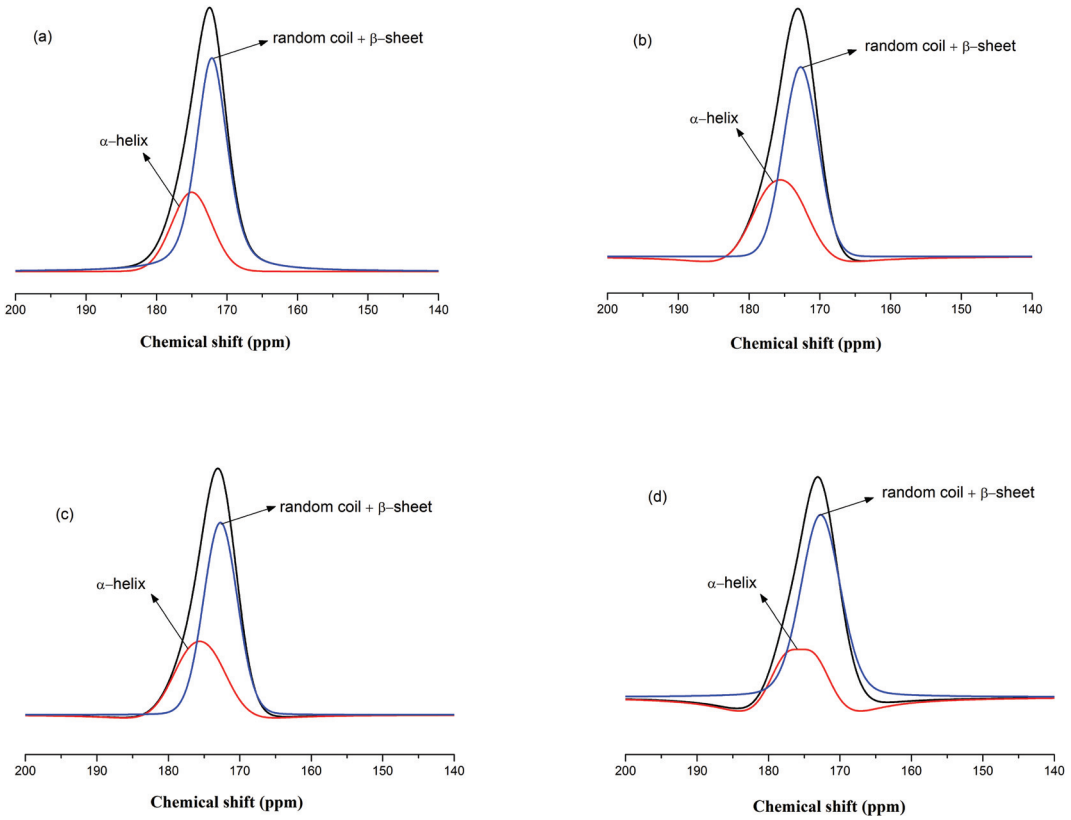

Fig. 8 The ^{13}C CP MAS NMR spectra of (a) raw material, (b) regenerated keratin material from [BMIM]Cl, (c) regenerated keratin material from [AMIM]Cl, and (d) regenerated keratin material from [choline][thioglycolate] which were fitted with Gaussian/Lorentzian fitting functions. The error in the fitting was ~3–5%.

α-helix, and the other at 172.7 ± 0.2 ppm which is related to the β-sheet molecular conformations, respectively.[43,44,46] However, another study ascribed the NMR peak at 172 ppm to the random coil structure as well.[47] Hence, we assume that the NMR peak ~172.0 ± 0.2 emerges from the nuclei of both β-sheet and random coil structures. In the present study, best fits for deconvoluting the carbonyl NMR peak for the raw material were achieved by using 175.0 ppm for the α-helix and 172.0 ppm for the random coil + β-sheet. On the other hand, for all of the regenerated materials, 175.6 ppm and 172.7 ppm respectively gave the best fits. Table 1 shows that, in the case of the raw and regenerated materials from [BMIM]Cl and [AMIM]Cl, the percentage fraction of the random coil + β-sheet was about double that of the α-helix and was unchanged in the regenerated material. Conversely, the percentage fraction of the random coil + β-sheet was much higher in the regenerated keratin from [choline][thioglycolate]. A plausible explanation of this observation is that the dissolution of turkey feather in reducing ionic liquids such as [choline][thioglycolate] results in a much stronger cleavage of the disulfide linkages and therefore promotes the formation of random coil and β-sheet structures. The NMR data in Table 1, which display a lesser fraction of the α-helix compared to the random coil + β-sheet for all materials, agree well with their corresponding X-ray diffraction spectra that also show a lesser fraction of the α-helix compared to the random coil + β-sheet.

Table 1 The percentage fraction of α-helix and random coil + β-sheet of raw material and regenerated keratin material, which were fitted using dmfit[a] program ^{13}C CP MAS NMR spectra

Peaks	% Fraction ± 5	Chemical shift (ppm) ± 0.2	FWHM (Hz) ± 20
Raw material			
α Helix	33	175.0	470
Random coil + β sheet	67	172.0	379
Regenerated keratin material from [BMIM]Cl			
α Helix	33	175.6	617
Random coil + β sheet	67	172.7	437
Regenerated keratin material from [AMIM]Cl			
α Helix	33	175.6	588
Random coil + β sheet	67	172.7	419
Regenerated keratin material from [choline][thioglycolate]			
α Helix	11	175.6	559
Random coil + β sheet	89	172.7	494

[a] The dmfit program was used for the deconvolution of NMR into various peaks and simulated fit.[45]

Thermal stability and phase behaviour

The thermal decomposition analyses of the raw material and regenerated keratin material were conducted by TGA (Fig. 9). Thermal stability of raw material and regenerated keratin showed that these materials were stable up to 200 °C, with the stability of regenerated keratin material being slightly higher

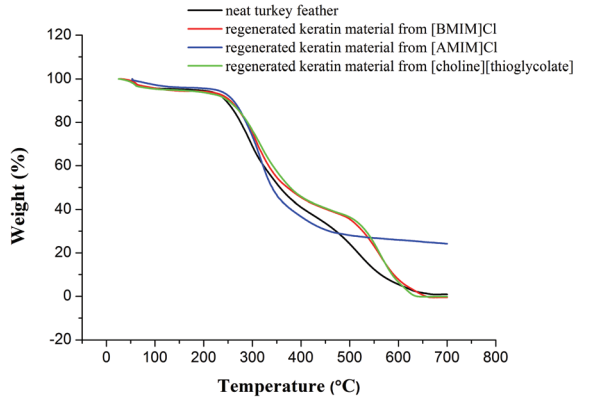

Fig. 9 Single heating scan TGA traces of keratin samples.

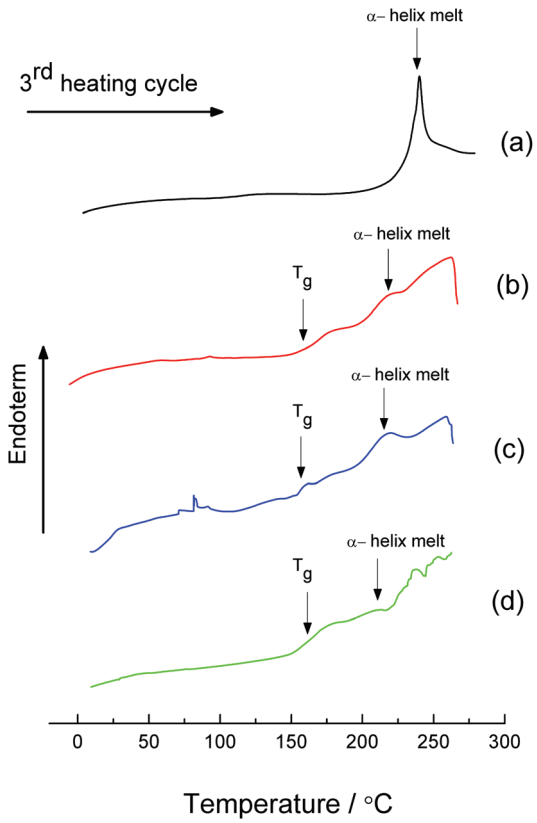

Fig. 10 DSC heating scan (3rd cycle) for (a) raw material and regenerated keratin material from (b) [BMIM]Cl, (c) [AMIM]Cl, and (d) [choline]-[thioglycolate].

than the raw turkey feather. There are two stages of decomposition that can be seen in all cases. A small weight loss involved in the first stage could be due to the evaporation of incorporated water near100 °C. Between 250 °C and 400 °C, the second stage involved with the degradation of the keratin materials.[10]

The phase behaviour of the keratin materials was studied by a differential scanning calorimeter (DSC). In order to ensure that no moisture was present in the samples, three consecutive heating and cooling cycles were carried out; the DSC traces in Fig. 10 are reported for the 3rd heating cycle. The DSC trace for the raw material {Fig. 10(a)} shows an exothermic peak around ~230 °C, which is usually assigned to α-helix disordering and decomposition (in some cases described as a "melt").[1] In the case of the regenerated keratin materials {Fig. 10(b)–(d)}, this peak was broadened and shifted to comparatively lower temperatures. These observations suggest the formation of some greater degree of disordered/amorphous phase and loss of the α-helix in all regenerated keratin materials compared to the raw keratin material. No obvious glass transition (T_g) was observed in the raw keratin material {Fig. 10(a)}, however in all regenerated materials, a prominent T_g was observed *ca.* 170 °C–180 °C. This tends to confirm the suggestion that these materials contain a higher degree of disordered material.

Characterisation of water soluble fraction

The development of methods to separate the water soluble fraction from the IL–water solution are underway and will be reported in a future publication. However, it was possible to gain some insight into the nature of the aqueous components as follows.

Sodium dodecyl sulphate-polyacrylamide gel electrophoresis (SDS-PAGE) analysis with a standard marker was employed to characterise and identify proteins in the water soluble fraction obtained during the regeneration of the keratin material. The protein bands were visualised by silver staining (Fig. 11). The presence of protein was confirmed and the majority of these proteins were in the molecular weight fraction range between 10 and 40 kDa. This observation indicates that upon dissolution in these three ionic liquids, there are proteins isolated that are water soluble. As 90% of the protein in feather samples is predicted to be keratin,[7] it is most likely that these water soluble polypeptides are keratin related fragments. The

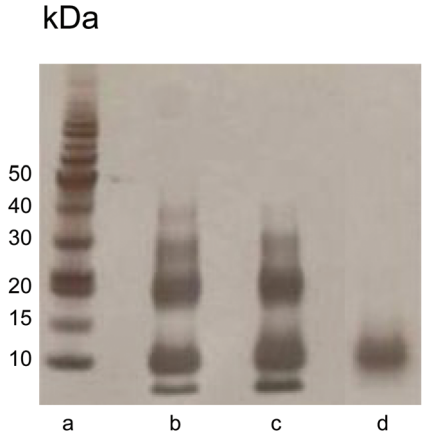

Fig. 11 SDS-PAGE pattern of (a) protein standard (b) water soluble protein in [BMIM]Cl, (c) water soluble protein in [AMIM]Cl, and (d) water soluble protein in [choline][thioglycolate].

most intense bands appeared at 10 kDa and 20 kDa in the [BMIM]Cl and [AMIM]Cl samples, whereas in [choline][thioglycolate] only one band appeared, at about ~10 kDa. The discreet bands differing by 10 kDa each are suggestive of monomeric, dimeric and possibly trimeric forms of the same protein sequence. This possibility is fuller supported by the disappearance of the longer multimeric fragments in the [choline][thioglycolate] that is thought to act as a reducing agent {Fig. 11(d)}. In addition, as the molecular weight of feather keratin monomer is ~10 kDa,[13,37,48] it is likely that these bands are representative of keratin monomer and dimers.

Conclusions

In summary, the solubility of feather keratin in ionic liquids is dependent on the ability of the anion and cation combination to disrupt the hydrogen bonding in the material. Several ionic liquids were shown to have good potential to be applied as solvents for feather dissolution. In particular, it was found that at 130 °C, turkey feather keratin is soluble in [BMIM]Cl, [AMIM]Cl and [choline][thioglycolate] up to 45 wt%. A regenerated keratin material representing up to 51% of the starting mass was obtained by precipitation from water. By ATR-FTIR, XRD and solid state NMR, it was observed that dissolution occurs without major chemical change of the polypeptide chain conformation, but did involve breakdown of the polymer chains into smaller segments and loss of some of the α-helix structure. The thioglycolate IL appeared to accelerate dissolution somewhat, causing a greater degree of fragmentation in the water soluble fraction and a greater degree of disruption of the α-helix structure, however it is clear that such a reducing agent is not a necessary component in dissolution. From the gel electrophoresis results, it was shown that the water soluble fraction is of lower molecular weight but still substantially polymeric. Further experimental studies of mechanical properties of a regenerated keratin biomaterial are in progress to evaluate the possibility of processing it into physical states such as fibers or films using known techniques.

Acknowledgements

The financial support from the Australian Research Council and DRM's Federation Fellowship is gratefully acknowledged.

Notes and references

1 J. Cao, *Thermochim. Acta*, 1999, **335**, 5–9.
2 M. Zoccola, A. Aluigi, C. Vineis, C. Tonin, F. Ferrero and M. G. Piacentino, *Biomacromolecules*, 2008, **9**, 2819–2825.
3 M. Zoccola, A. Aluigi and C. Tonin, *J. Mol. Struct.*, 2009, **938**, 35–40.
4 H. Xie, S. Li and S. Zhang, *Green Chem.*, 2005, **7**, 606–608.
5 S. Huda and Y. Yang, *J. Polym. Environ.*, 2009, **17**, 131–142.
6 A. A. Onifade, N. A. Al-Sane, A. A. Al-Musallam and S. Al-Zarban, *Bioresour. Technol.*, 1998, **66**, 1–11.
7 N. Reddy and Y. Yang, *J. Polym. Environ.*, 2007, **15**, 81–87.
8 K. M. Arai, R. Takahashi, Y. Yokote and K. Akahane, *Eur. J. Biochem.*, 1983, **132**, 501–507.
9 R. D. B. Fraser, *Keratins: Their Composition, Structure, and Biosynthesis*, 1972.
10 A. Ullah, T. Vasanthan, D. Bressler, A. L. Elias and J. Wu, *Biomacromolecules*, 2011, **12**, 3826–3832.
11 K. Yamauchi, A. Yamauchi, T. Kusunoki, A. Kohda and Y. Konishi, *J. Biomed. Mater. Res.*, 1996, **31**, 439–444.
12 E.-K. Bang, M. Lista, G. Sforazzini, N. Sakai and S. Matile, *Chem. Sci.*, 2012, **3**, 1752–1763.
13 A. J. Poole, J. S. Church and M. G. Huson, *Biomacromolecules*, 2008, **10**, 1–8.
14 H. J. Rodhes, B. Potter and A. Widra, *Mycopathol. Mycol. Appl.*, 1967, **33**, 345.
15 R. Cecil and J. R. McPhee, *Adv. Protein Chem.*, 1959, **14**, 255–389.
16 R. S. Asquith and N. H. Leon, *Chemical reactions of keratin fibres*, 1977.
17 J. A. Maclaren, *Aust. J. Chem.*, 1962, **15**, 824.
18 S. A. Forsyth, J. M. Pringle and D. R. MacFarlane, *Aust. J. Chem.*, 2004, **57**, 113–119.
19 D. R. MacFarlane and K. R. Seddon, *Aust. J. Chem.*, 2007, **60**, 3–5.
20 U. Domańska and R. Bogel-Łukasik, *J. Phys. Chem. B*, 2005, **109**, 12124–12132.
21 M. G. Freire, L. M. N. B. F. Santos, A. M. Fernandes, J. A. P. Coutinho and I. M. Marrucho, *Fluid Phase Equilib.*, 2007, **261**, 449–454.
22 R. P. Swatloski, S. K. Spear, J. D. Holbrey and R. D. Rogers, *J. Am. Chem. Soc.*, 2002, **124**, 4974–4975.
23 A. Biswas, R. L. Shogren, D. G. Stevenson, J. L. Willett and P. K. Bhowmik, *Carbohydr. Polym.*, 2006, **66**, 546–550.
24 M. Zavrel, D. Bross, M. Funke, J. Büchs and A. C. Spiess, *Bioresour. Technol.*, 2009, **100**, 2580–2587.
25 S. S. Y. Tan, D. R. MacFarlane, J. Upfal, L. A. Edye, W. O. S. Doherty, A. F. Patti, J. M. Pringle and J. L. Scott, *Green Chem.*, 2009, **11**, 339–345.
26 C. Azubuike, H. Rodríguez, A. Okhamafe and R. Rogers, *Cellulose*, 2012, **19**, 425–433.
27 J. Gao, Z.-G. Luo and F.-X. Luo, *Carbohydr. Polym.*, 2012, **89**, 1215–1221.
28 M. E. Zakrzewska, E. Bogel-Lukasik and R. Bogel-Lukasik, *Energy Fuels*, 2010, **24**, 737–745.
29 L. Zhao, Y. X. Tang, R. F. Zhao, W. K. Mao, S. Chen and J. Hua, *Wool Textile J.*, 2010, **38**, 1–5.
30 G. Laus, G. Bentivoglio, H. Schottenberger, V. Kahlenberg, H. Kopacka, H. Roeder, T. Roeder and H. Sixta, *Lenzinger Berichte*, 2005, **84**, 71–85.
31 P. Nockemann, K. Binnemans and K. Driesen, *Chem. Phys. Lett.*, 2005, **415**, 131–136.
32 L. Mayrand-Provencher and D. Rochefort, *Electrochim. Acta*, 2009, **54**, 7422–7428.
33 A. L. Horvath, *Sci. World J.*, 2009, **9**, 255–271.

34 Z. Meng, X. Zheng, K. Tang, J. Liu, Z. Ma and Q. Zhao, *Int. J. Biol. Macromol.*, 2012, **51**, 440–448.
35 J. M. Gillespie and F. G. Lennox, *Biochim. Biophys. Acta*, 1953, **12**, 481–482.
36 J. Stoimenovski, E. I. Izgorodina and D. R. MacFarlane, *Phys. Chem. Chem. Phys.*, 2010, **12**, 10341–10347.
37 P. M. M. Schrooyen, P. J. Dijkstra, R. G. Oberthü, A. Bantjes and J. Feijen, *J. Agric. Food Chem.*, 2000, **48**, 4326–4334.
38 C. B. Jones and D. K. Mecham, *Arch. Biochem.*, 1943, **3**, 193–202.
39 E. Wojciechowska, A. Wlochowicz and A. Weselucha-Birczynska, *J. Mol. Struct.*, 1999, **511–512**, 307–318.
40 R. Schor and S. Krimm, *Biophys. J.*, 1961, **1**, 467–487.
41 R. Meredith, *The Mechanical Properties of Textile Fibres*, 1956.
42 D. R. Rao and V. B. Gupta, *J. Appl. Polym. Sci.*, 1992, **46**, 1109–1112.
43 C. M. Carr and W. V. Germasimowicz, *Text. Res. J.*, 1988, **58**, 418–421.
44 M. J. Duer, N. McDougal and R. C. Murray, *Phys. Chem. Chem. Phys.*, 2003, **5**, 2894–2899.
45 D. Massiot, F. Fayon, M. Capron, I. King, S. Le Calvé, B. Alonso, J. O. Durand, B. Bujoli, Z. Gan and G. Hoatson, *Magn. Reson. Chem.*, 2002, **40**, 70–76.
46 M. Baias, D. E. Demco, C. Popescu, R. Fechete, C. Melian, B. Blümich and M. Möller, *J. Phys. Chem. B*, 2009, **113**, 2184–2192.
47 N. Nishikawa, Y. Tanizawa, S. Tanaka, Y. Horiguchi and T. Asakura, *Polymer*, 1998, **39**, 3835–3840.
48 A. M. Woodin, *Biochem. J.*, 1954, **57**, 99–109.

